Magnetic phase transitions of $CrCl_3$ graphite intercalation compound

Masatsugu Suzuki and Itsuko S. Suzuki
Department of Physics, State University of New York at Binghamton, Binghamton, New York 13902-6016
(Received 2 September 1997)

Magnetic phase transitions of stage-2 $CrCl_3$ graphite intercalation compound have been studied using ac superconducting quantum interference device (SQUID) magnetic susceptibility and dc SQUID magnetization. This compound is a two-dimensional (2D) Heisenberg ferromagnet with small XY anisotropy and very weak antiferromagnetic interplanar exchange interaction: interplanar exchange interaction J $(=5.86\pm0.05$ K), effective anisotropy field $H_A^{\rm out}(=193$ Oe), and $H_E'(=51$ Oe). This compound undergoes magnetic transitions at $T_{c1}(=11.5$ K), $T_{c2}(=10.3-10.5$ K), $T_{c3}(=8.67-9.70$ K), and $T_g(=5.7-7$ K). Below T_{c1} a 2D ferromagnetic long-range order with spin component along the c axis appears, forming an axial ferromagnetic phase. Below T_{c2} a 2D ferromagnetic long-range order of spin component perpendicular to the c axis appears, forming an oblique phase. Below T_{c3} there appears a 3D antiferromagnetic order accompanying spin-glass-like behavior. Below T_g the system enters into a reentrant spin glass phase arising from the competition between a ferromagnetic Cr^{3+}-Cr^{3+} interaction and possible antiferromagnetic Cr^{2+}-Cr^{2+} interactions. The role of Cr^{2+} spins with Ising symmetry may be crucial for the axial ferromagnetic and oblique phases.
[S0163-1829(98)02218-8]

I. INTRODUCTION

Magnetic binary graphite intercalation compounds (GIC's) provide a model system for studying magnetic phase transitions of two-dimensional (2D) spin systems.[1,2] The magnetic dimensionality of GIC's can be controlled by varying the stage number, the number of graphite layers between adjacent magnetic intercalate layers. The intraplanar exchange interactions are almost the same as those of their pristine forms, while the interplanar exchange interactions are dramatically decreased with increasing stage number. Among these GIC's it is well known that stage-2 $CoCl_2$ GIC magnetically behaves like a 2D XY-like ferromagnet on the triangular lattice.[1,2] So far, a considerable amount of work has been done on the magnetic phase transition of this compound. Detailed magnetic measurements including neutron scattering indicate successive transitions with a 2D long-range spin order in the intermediate phase.

In this paper we study the magnetic phase transitions of stage-2 $CrCl_3$ GIC. In contrast to stage-2 $CoCl_2$ GIC, there has been very little work on the magnetic properties of stage-2 $CrCl_3$ GIC, partly because of the difficulty in preparing this compound with a well-defined staging structure. We show that stage-2 $CrCl_3$ GIC magnetically behaves like a 2D Heisenberg ferromagnet with very small XY anisotropy (see Sec. IV A). Cr^{3+} ions with spin $S(=3/2)$ are located on the honeycomb lattice of the intercalate layers. Here we examine the magnetic properties of stage-2 $CrCl_3$ GIC based on highly oriented pyrolytic graphite (HOPG) using ac superconducting quantum interference device (SQUID) magnetic susceptibility and dc SQUID magnetization measurements along the c plane (perpendicular to the c axis) and the c axis. The effect of an external magnetic field on the phase transitions is also examined. Like stage-2 $CoCl_2$ GIC, stage-2 $CrCl_3$ GIC undergoes successive magnetic phase transitions. However, the details of the phase transitions in stage-2 $CrCl_3$ GIC are different from those of stage-2 $CoCl_2$ GIC. Several different kinds of long-range spin order occur in this compound, including a 2D axial ferromagnetic phase, a 2D oblique phase, a 3D antiferromagnetic phase, and a reentrant spin glass phase. The nature of these ordered phases is discussed (Secs. IV B and IV C).

Pristine $CrCl_3$ has a hexagonal layered-type crystal structure. The magnetic properties of $CrCl_3$ have been reported in detail.[3–9] Pristine $CrCl_3$ undergoes a magnetic phase transition below 16.8 K to an antiferromagnetic state and similarly to $CoCl_2$ and $NiCl_2$, with the spin directions lying in the c plane and forming ferromagnetic layers which alternate in direction along the c axis. The magnetic structure of $CrCl_3$ is indicative of a ferromagnetic interaction within the metal ion layers and an antiferromagnetic interaction between layers. The in-plane structure of the $CrCl_3$ intercalate layer in stage-2 $CrCl_3$ GIC is the same as that of pristine $CrCl_3$, while the interplanar distance between adjacent $CrCl_3$ layers greatly increases from 5.78 to 12.80 Å on intercalation.[10] This suggests that the ferromagnetic intraplanar exchange interaction J remains unchanged, but that the magnitude of antiferromagnetic interplanar exchange interaction $J'(<0)$ is greatly reduced upon intercalation. There have been several works on the magnetic properties of mainly stage-3 $CrCl_3$ GIC using dc magnetic susceptibility, magnetization, nonlinear magnetic susceptibility, and electron spin resonance experiments. Here we present a simple review of the magnetic phase transitions of stage-3 $CrCl_3$ GIC.[11–15] A zero-field-cooled magnetization $M_{\rm ZFC}$ in the presence of an external magnetic field $H(=2$ Oe) along the c plane shows a single peak around 10 K, while a field-cooled magnetization $M_{\rm FC}$ has an inflection point at 11.3 ± 0.2 K and drastically increases with decreasing temperature between 10 and 12 K. The deviation of $M_{\rm ZFC}$ from $M_{\rm FC}$ occurs below 11.3 K.[12] The nonlinear magnetic susceptibility χ_2 shows a sharp peak at 11.4 K and changes its sign at 9.7 K. Here χ_2 is defined by $\chi_2=-4M'(3\omega)/h^3$ in the limit of $h\to0$ and $\omega\to0$, where

$M'(3\omega)$ is a real part of third harmonic in-phase component of ac magnetization and h is the amplitude of ac magnetic field with angular frequency ω.[11]

II. EXPERIMENTAL PROCEDURE

A stage-2 $CrCl_3$ GIC sample was prepared by heating a mixture of anhydrous $CrCl_3$ and HOPG sealed in a vacuum in a quartz tubing. The reaction was made at 850 °C for 1 month. The stoichiometry of this compound is determined as $C_{20.9}CrCl_3$ from weight uptake measurements. The stage number of this compound was confirmed from (00L) x-ray diffraction to be well-defined stage 2 with a c-axis repeat distance of 12.80 ± 0.02 Å. The sample used in the magnetic measurement has a rectangular form with a base 2.60 mm×3.81 mm and a thickness of 0.64 mm along the c axis.

The ac magnetic susceptibility and dc magnetization were measured using a SQUID magnetometer (Quantum Design, MPMS XL-5) with a ultralow-field capability option. (i) ac magnetic susceptibility: The sample was cooled from 298 to 1.9 K in a zero magnetic field (less than 3 mOe). Then the temperature (T) dependence of dispersion χ' and absorption χ'' was measured between 1.9 and 18 K in the absence and presence of H. The amplitude of the ac magnetic field h is 50 mOe, and the frequency (f) range is between 0.1 Hz and 1 kHz. (ii) dc magnetization: The sample was cooled from 298 to 1.9 K in a zero magnetic field. Then an external magnetic field H ($=1$ Oe) is applied at 1.9 K. The zero-field-cooled magnetization ($M_{\rm ZFC}$) was measured with increasing temperature from 1.9 to 25 K, and the field-cooled magnetization ($M_{\rm FC}$) was measured with decreasing temperature from 25 to 1.9 K. (iii) The dc magnetic susceptibility was also measured while the sample was cooled from 300 to 2 K in the presence of $H(=1$ kOe).

The intrinsic susceptibility $\chi_{\rm in}$ in units of emu/mol is related to the measured one χ_e by $\chi_{\rm in}=\chi_e/(1-NA\chi_e)$, where N is the demagnetizing factor and A is a factor defined by the density ρ divided by the molar mass of the stoichiometry $C_{20.9}CrCl_3$, and ρ is calculated as 1.94 g/cm^3. The value of A is estimated as 4.74×10^{-3}. We assume that the demagnetizing factor N is equal to 4π and 0 parallel and perpendicular to the c axis. Here the data for $H\|c$ are presented without correction of the demagnetizing effect.

III. RESULT

A. dc magnetic susceptibility

We have measured the dc magnetic susceptibility of stage-2 $CrCl_3$ GIC based on HOPG in the presence of H ($=1$ kOe) along the c plane and c axis. We find that the dc magnetic susceptibility along the c plane, χ_a, obeys a Curie-Weiss law in the temperature range $50\leqslant T\leqslant300$ K. The least squares fit of the data to

$$\chi_i=\frac{C_i}{T-\Theta_i}+\chi_i^0 \quad (i=a \text{ and } c) \tag{1}$$

yields the Curie-Weiss temperature $\Theta_a=24.05\pm0.05$ K and the Curie-Weiss constant $C_a=1.388\pm0.002$ emu K/mol. Figure 1(a) shows the reciprocal magnetic susceptibility

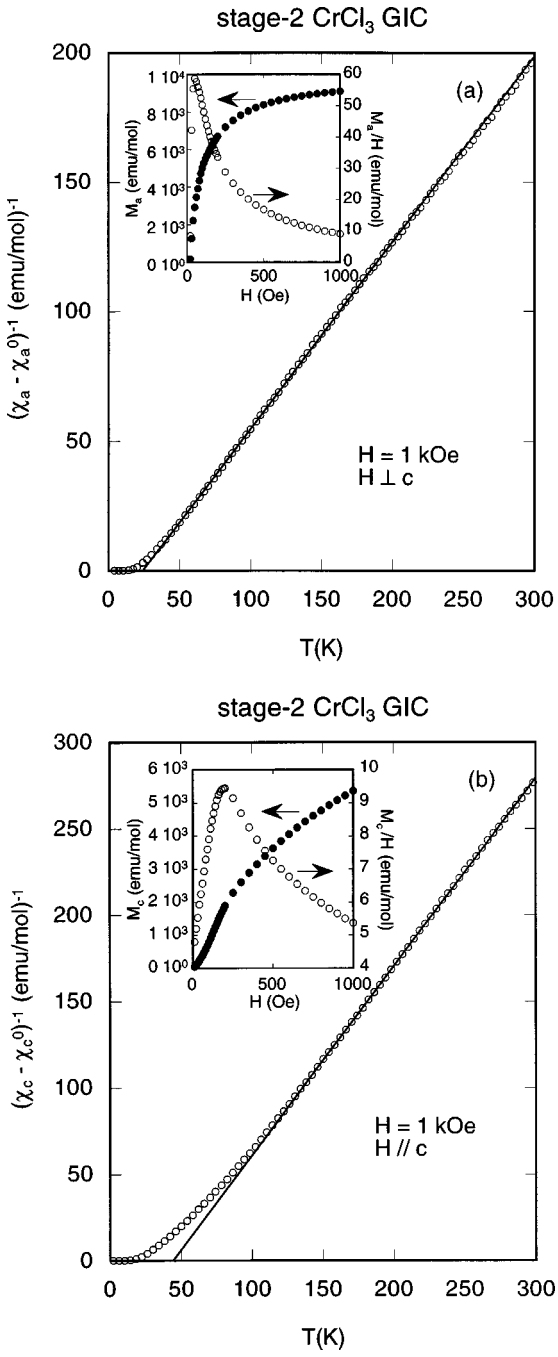

FIG. 1. Reciprocal dc magnetic susceptibility $(\chi_i-\chi_i^0)^{-1}$ vs T for stage-2 $CrCl_3$ GIC. $H=1$ kOe. (a) $i=a$ ($H\perp c$) and (b) $i=c$ ($H\|c$). The inset shows the field dependence of magnetization M_i and dc magnetic susceptibility χ_i ($=M_i/H$) at 1.9 K.

$(\chi_a-\chi_a^0)^{-1}$ of stage-2 $CrCl_3$ GIC as a function of temperature. The deviation of data from a straight line exhibiting the Curie-Weiss law becomes appreciable below 30 K, implying the growth of short-range spin order. This result is consistent with the electron spin resonance result of stage-3 $CrCl_3$ GIC that the linewidth divergingly increases with decreasing temperature below 35 K.[13–15] The value of Θ_a is close to that reported by Chehab *et al.*[13] ($\Theta_a=26$ K) for stage-3 $CrCl_3$ GIC. The effective magnetic moment $P_{\rm eff}^{(a)}$ is calculated from the value of C_a as $P_{\rm eff}^{(a)}=(3.332\pm0.005)\mu_B$, which is relatively smaller than $3.87\mu_B$ for the complete quenching of

orbital angular momentum: $P_{\rm eff}=2[S(S+1)]$, with $S=3/2$. Here we note that the value of $P_{\rm eff}$ for pristine $CrCl_3$ is estimated as $3.90\mu_B$ from the dc magnetic susceptibility[3] and as 2.72 ± 0.10 for $L=3$, 3.04 ± 0.20 for $L=9$, and 3.20 ± 0.40 for $L=15$ from the intensities of the (00L) antiferromagnetic Bragg reflection in magnetic neutron scattering.[5] The positive Θ_a indicates that the intraplanar exchange interaction is ferromagnetic. The intraplanar ferromagnetic exchange interaction is estimated as $J=3.21\pm0.01$ K from the relation $\Theta=2zJS(S+1)/3$, where $z(=3)$ is the number of nearest-neighbor Cr atoms. This value of J is much smaller than that of pristine $CrCl_3$ ($J=5.25$ K) obtained from the spin wave analysis.[6]

The dc magnetic susceptibility along the c axis, χ_c, obeys the Curie-Weiss law in the temperature range $150\leqslant T\leqslant300$ K. The least squares fit of the data to Eq. (1) yields $\Theta_c=43.94\pm0.67$ K and $C_c=0.916\pm0.008$ emu K/mol. Even if the demagnetizing effect is taken into account, the values of Θ_c and C_c do not change at all. Figure 1(b) shows the reciprocal magnetic susceptibility $(\chi_c-\chi_c^0)^{-1}$ of stage-2 $CrCl_3$ GIC as a function of temperature. The value of $P_{\rm eff}^{(c)}$ is estimated as $P_{\rm eff}^{(c)}=(2.71\pm0.12)\mu_B$, which is much smaller than $P_{\rm eff}^{(a)}$, but is in agreement with that estimated from the intensity of (003) antiferromagnetic Bragg reflection in $CrCl_3$.[5] Note that the value of Θ_c is very different from that reported by Chehab *et al.*[13] ($\Theta_c=25$ K) for stage-3 $CrCl_3$ GIC. The value of J is estimated as $J=5.86\pm0.09$ K from $\Theta_c(=43.94$ K), which is a little larger than that of pristine $CrCl_3$ ($J=5.25$ K). Since the in-plane structure remains unchanged on intercalation, it may be reasonable to assume that the value of J does not change so much. So we adhere to the value of $J(=5.86$ K).

The insets of Figs. 1(a) and 1(b) show the field dependence of magnetization M_a and dc magnetic susceptibility $\chi_a(=M_a/H)$ and M_c and χ_c at 1.9 K, respectively. The susceptibility χ_a has a sharp peak at $H=60$ Oe corresponding to a spin flop field $H_{\rm SF}$, while χ_c has a broad peak around $H=200$ Oe corresponding to the XY-symmetry-preserving field $H_A^{\rm out}$ (see Sec. IV A for details). The value of $M_a(=9.1\times10^3$ emu/mol) at $H=1$ kOe is still relatively smaller than the saturation magnetization described by $M_s^{(a)}=N_A g_a\mu_B S=(5.585\times10^3)g_a S=1.675\times10^4$ (emu/mol) for $g_a\approx2$, where N_A is the Avogadro number. The value of M_c is smaller than that of M_a, indicating the XY spin symmetry of this system.

B. $M_{\rm ZFC}$ and $M_{\rm FC}$

Figure 2(a) shows the T dependence of the magnetization $M_{\rm ZFC}^a$ and $M_{\rm FC}^a$ along the c plane when $H(=1$ Oe) is applied along the c plane. The magnetization $M_{\rm ZFC}^a$ has a broad peak at 10.1 K and a shoulder at 11.5 K. The deviation of $M_{\rm FC}^a$ from $M_{\rm ZFC}^a$ occurs below 12.1 K, indicating an irreversible effect of magnetization.

Figure 2(b) shows the T dependence of $M_{\rm ZFC}^c$ and $M_{\rm FC}^c$ along the c axis when $H(=1$ Oe) is applied along the c axis. No correction of demagnetization is taken for this data. The magnetization $M_{\rm ZFC}^c$ has a peak at 10.5 K and a shoulder at 11.5 K. The deviation of $M_{\rm FC}^c$ from $M_{\rm ZFC}^c$ occurs below 12.1 K. The magnetization $M_{\rm FC}^c$ drastically increases around 12 K with decreasing temperature, showing a very broad peak around 5.2 K. With further decreasing temperature, $M_{\rm FC}^c$ slightly decreases.

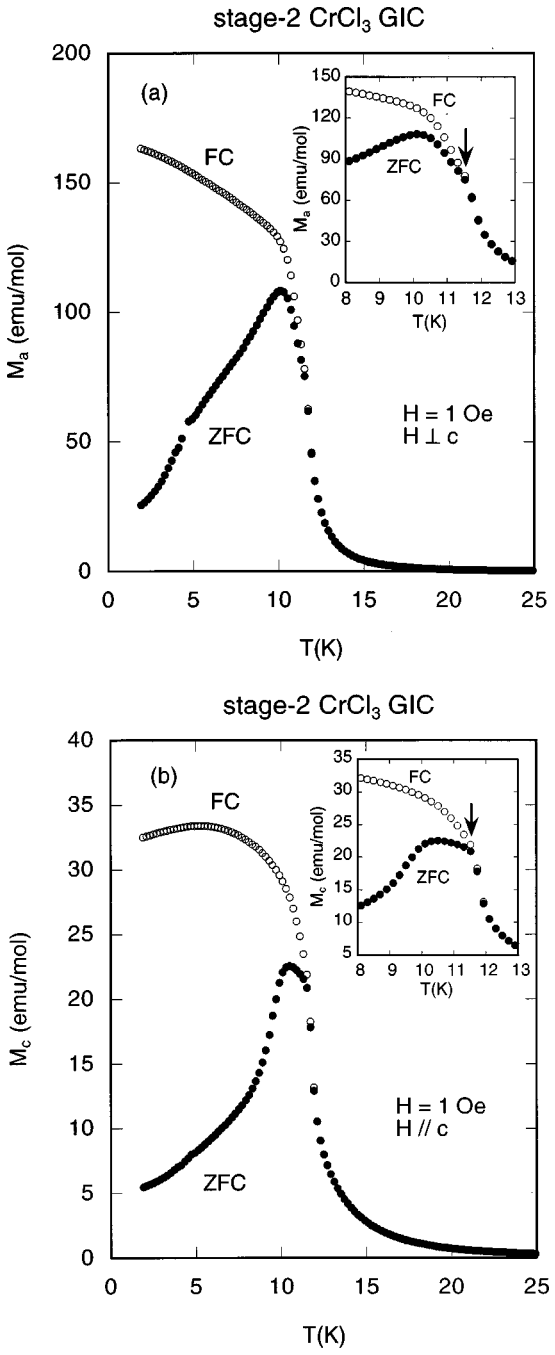

FIG. 2. T dependence of $M_{\rm FC}$ and $M_{\rm ZFC}$ (a) along the c plane ($H\perp c$) and (b) along the c axis ($H\parallel c$). $H=1$ Oe.

C. χ'_{aa} and χ''_{aa} at $H=0$

Figure 3 shows the T dependence of dispersion χ'_{aa} at various frequencies, where h is applied along the c plane. The dispersion χ'_{aa} has a peak at 10.3 K for $f=0.1$ Hz. This peak slightly shifts to the high temperature side with increasing frequency: 10.50 K at $f=1$ kHz. The dispersion χ'_{aa} has a shoulder at 11.5 K independent of frequency [see Fig. 8(a) for details]. Note that the magnitude of χ'_{aa} strongly depends on frequency at fixed temperatures below 11.5 K.

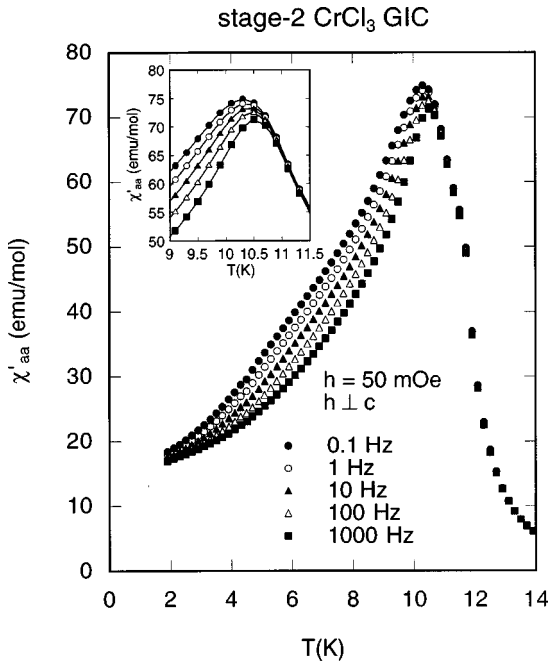

FIG. 3. T dependence of χ'_{aa} for various frequencies f ($=0.1-1000$ Hz). $h=50$ mOe. $h\perp c$. $H=0$. The inset shows a detail of χ'_{aa} vs T for $9\leqslant T\leqslant 11.5$ K.

Figure 4(a) shows the T dependence of absorption χ''_{aa} for various frequencies. The absorption χ''_{aa} has a peak at a temperature T_p ($=8.67$ K at $f=0.1$ Hz and 9.71 K for $f=1$ kHz) and a small peak at 11.5 K independent of frequency [see the inset of Fig. 4(a)]. The absorption χ''_{aa} for $0.1\leqslant f\leqslant 10$ Hz also has a plateaulike form in the temperature range between ≈ 6 K and T_p. In the inset of Fig. 4(b), we show the plot of T_p as a function of frequency. The peak temperature T_p monotonically increases with increasing frequency, suggesting the occurrence of a spin glass phase in this system. Here we assume that χ''_{aa} has a peak at $\omega\tau=1$ ($\omega=2\pi f$), where τ is an average relaxation time. In Fig. 4(b) we make the plot of τ vs T, showing a drastic increase of τ with decreasing temperature. The most likely source for such a divergence of τ is a critical slowing down near a critical temperature T^*. The least squares fit of these data to

$$\tau=\tau_0(T/T^*-1)^{-x} \tag{2}$$

yields $\tau_0=1.13\times 10^{-12}$ sec, $T^*=7.04\pm 1.37$ K, and $x=19.20\pm 12.82$, where τ_0 is a time constant, T^* is a critical temperature, and x is a dynamic critical exponent. The value of x is too large and is unphysical. The large uncertainty in x arises mainly from the limited number of data.

Figures 4(c) and 4(d) show the frequency dependence of absorption χ''_{aa} at various temperatures for $0.1\leqslant f\leqslant 1000$ Hz. The form of χ''_{aa} vs f depends on the temperatures: (i) χ''_{aa} decreases with increasing frequency ($1.9\leqslant T\leqslant 5.7$ K), (ii) it is almost independent of frequency around 5.9–6.1 K, (iii) it increases with increasing frequency, having a small local maximum around $f=1$ Hz ($6.3\leqslant T\leqslant 8.9$ K), (iv) it increases with increasing frequency ($9.1\leqslant T\leqslant 10.1$ K), and (v) it decreases with increasing frequency, having a local minimum around 10 Hz and, in turn, increasing with further increasing frequency ($10.3\leqslant T\leqslant 12.1$ K). We assume that χ''_{aa} may be described by a relaxation function

$$\chi''_{aa}\approx G(\omega\tau)=\frac{\sin[\pi(1-a)/2](\omega\tau)^{1-a}}{1+(\omega\tau)^{2(1-a)}+2\cos[\pi(1-a)/2](\omega\tau)^{1-a}}, \tag{3}$$

where $0\leqslant a<1$ and $a=0$ for the Debye-type relaxation. The relaxation function $G(\omega\tau)$ is proportional to $(\omega\tau)^{1-a}$ for $\omega\tau\ll 1$ and proportional to $(\omega\tau)^{-1+a}$ for $\omega\tau\gg 1$. The above result suggests that the average relaxation time τ divergingly increases with decreasing temperature below 5.9–6.1 K. The spin glass phase may occur below these temperatures. As is shown on the data at 4.7 K in Fig. 4(c), the broad spectral width of up to 4 decades in frequency full width at half maximum (FWHM) (compared to a single time Debye fixed width of 1.14 decades) reflects an extremely broad distribution of relaxation times: $a\approx 1$.

D. χ'_{aa} and χ''_{aa} at H

Figure 5(a) shows the T dependence of dispersion χ'_{aa} at various magnetic fields applied along the c plane, where $f=100$ Hz. The dispersion χ'_{aa} has a peak at $T_p(H=0)=10.50$ K at $H=0$. This peak of χ'_{aa} shifts to the high-temperature side and is smeared out with increasing magnetic field, implying that the in-plane ferromagnetic order is apparently enhanced by the application of H. In the inset we show the plot of T_p as a function of H. The peak height $\chi'_{\max}$ monotonically decreases as the magnetic field increases. The peak height is described by

$$\chi'_{\max}\approx H^{-\lambda}, \tag{4}$$

for $20\leqslant H\leqslant 1000$ Oe with $\lambda=0.855\pm 0.016$. The deviation of peak temperature $T_p(H)$ from $T_p(0)$ is well described by

$$T_p(H)-T_p(0)\approx H^{\mu}, \tag{5}$$

for $20\leqslant H\leqslant 1000$ Oe with exponent $\mu=0.524\pm 0.030$. In Fig. 5(b) we show a plot of the normalized susceptibility $\chi'_{aa}/\chi'_{\max}$ as a function of t/H^{μ} for $\mu=0.524$, where $t=T/T_p(H=0)-1$. Almost all the data above $T_p(H)$ seem to fall on a single-valued scaling function $\Phi(t/H^{\mu})$, while the data at temperatures between $T_p(0)$ and $T_p(H)$ are rather scattered. Similar behaviors are observed in K_2CuF_4: $\mu=0.83\pm 0.05$ and $\lambda=0.82\pm 0.05$.[16] Thus the dispersion χ'_{aa} for $T>T_p(H)$ is expressed by

$$\chi'_{aa}\approx H^{-\lambda}\Psi(H/t^{1/\mu}), \tag{6}$$

where $\Phi(t/H^{\mu})=\Phi((H/t^{1/\mu})^{-\mu})=\Psi(H/t^{1/\mu})$. This scaling form coincides with a conventional scaling form for the static susceptibility when $\beta=(1-\lambda)/\mu$ and $\gamma=\lambda/\mu$, where β and γ are the critical exponents for spontaneous magnetization and magnetic susceptibility, respectively. The values of β and γ are estimated as $\beta=0.28\pm 0.01$ and $\gamma=1.63\pm 0.02$, respectively. These exponents are in good agreement with those of the 2D XY-like ferromagnet K_2CuF_4 for $t\geqslant 7\times 10^{-2}$: $\beta=0.33$ from neutron scattering[17] and $\gamma=1.7-1.9$ from ac magnetic susceptibility.[18]

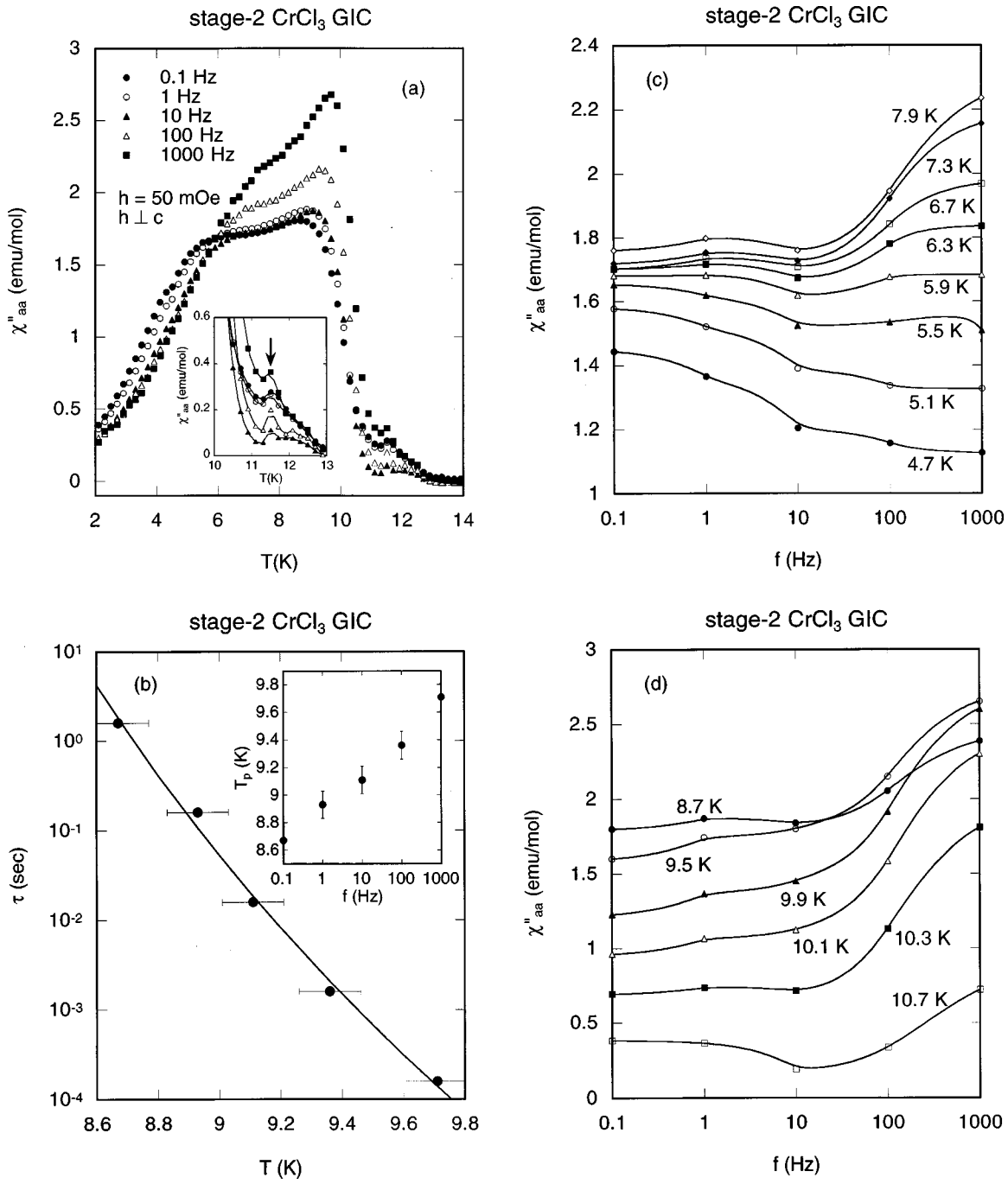

FIG. 4. (a) T dependence of χ''_{aa} for various frequencies f, where $h=50$ mOe, $h\perp c$, and $H=0$. The inset shows a detail of χ''_{aa} vs T for $10\leqslant T\leqslant 13$ K. (b) Average relaxation time τ vs T derived from the relation of peak temperature vs frequency shown in the inset. (c) and (d) Frequency dependence of χ''_{aa} for various temperatures.

Figure 5(c) shows the T dependence of absorption χ''_{aa} at various magnetic fields applied along the c plane, where $f=100$ Hz. The absorption χ''_{aa} has a broad peak at 9.30 K and a shoulder around 6.7 K for $H=0$. For $H=5$ Oe this shoulder changes into a broad peak at 6.9 K, which shifts to the low-temperature side with increasing field: 6.48 K for $H=50$ Oe. The peak completely disappears above 70 Oe. Such a decrease of peak temperature with H may be related to the Almeida-Thouless transition: the spin glass freezing temperature decreases with increasing H. In contrast, the broad peak at 9.30 K for $H=0$ Oe shifts to the high-temperature side with increasing field: 10.32 K for $H=50$ Oe. This behavior is related to the appearance of an in-plane ferromagnetic state which is enhanced by the application of H along the c plane.

E. χ'_{cc} and χ''_{cc} at $H=0$

Figure 6(a) shows the T dependence of dispersion χ'_{cc} at various frequencies, where h is applied along the c axis. The absorption χ'_{cc} has a sharp peak at 11.5 K independent of frequency. This peak temperature coincides with a tempera

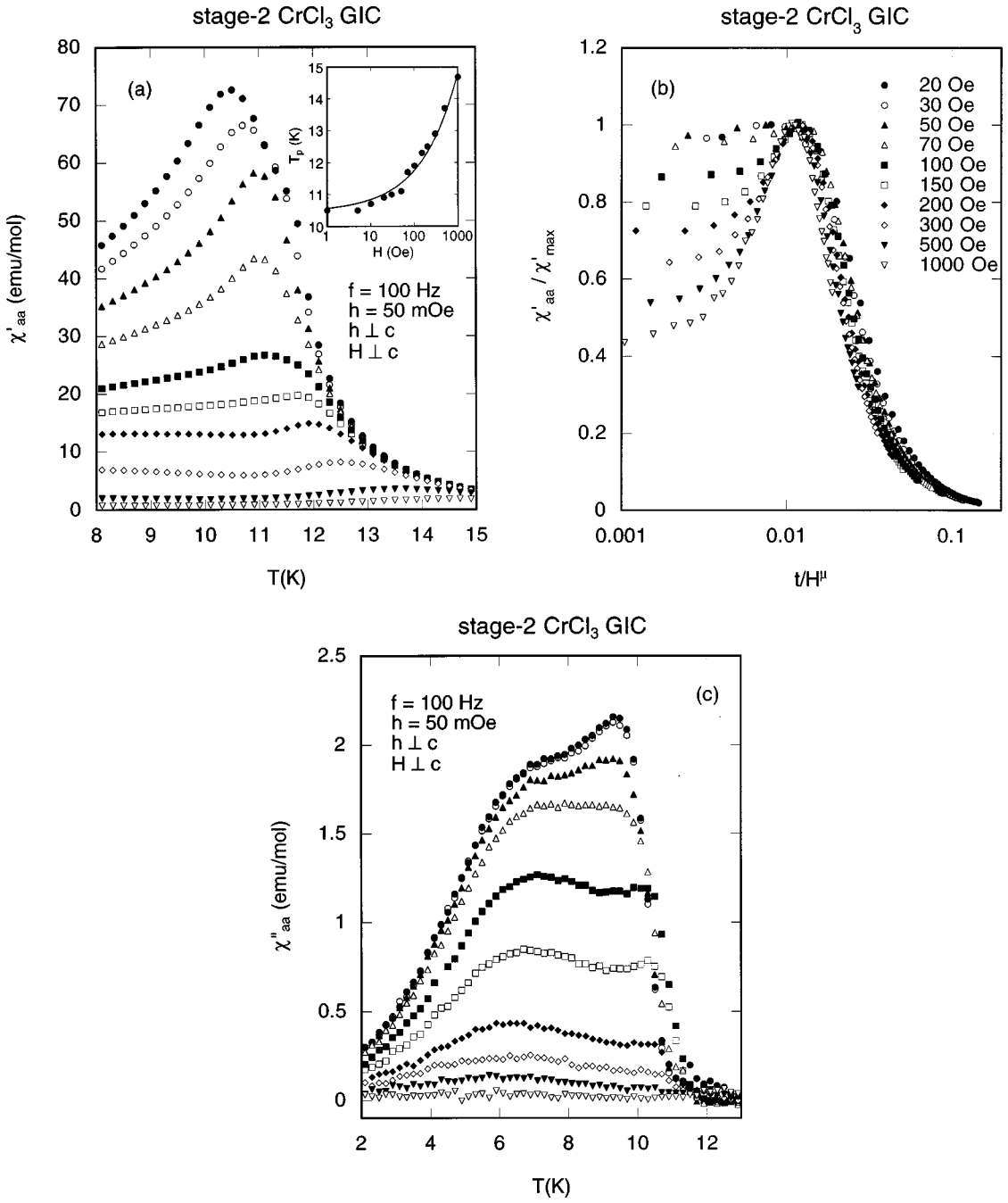

FIG. 5. (a) T dependence of χ'_{aa} for various magnetic fields H ($\perp c$), where $f=100$ Hz, $h=50$ mOe, and $H=0$ (●), 10 (○), 20 (▲), 30 (△), 50 (■), 70 (□), 100 (♦), 200 (◇), 500 (▼), and 1000 (▽) Oe. The inset shows the plot of peak temperature T_p vs H. (b) Scaling plot of $\chi'_{aa}/\chi'_{\max}$ vs t/H^{μ} for various H where $t=T/T_p(H=0)-1$, $T_p(0)=10.50$ K, and $\mu=0.524$. (c) T dependence of χ''_{aa} for various magnetic fields H ($\perp c$), where $f=100$ Hz, $h=50$ mOe, and $H=0$ (●), 1 (○), 5 (▲), 10 (△), 20 (■), 30 (□), 50 (♦), 70 (◇), 100 (▼), and 200 (▽) Oe.

ture where χ''_{aa} has a small peak and χ'_{aa} has a shoulder. It also agrees well with that ($T=11.4$ K) obtained from the nonlinear magnetic susceptibility χ_2. These results suggest that the transverse component (along the c axis) of spins orders below 11.5 K, forming an axial ferromagnetic phase (see Sec. IV C). The dispersion χ'_{cc} is smaller than χ'_{aa} below 18 K, which is the highest temperature in the present measurement. Here we note a possibility that χ'_{cc} may be simply a part of χ'_{aa} because of misalignment or mosaic spread of the sample. However, this is not the case for our system: the magnitude of χ'_{cc} is much larger than that estimated based on this possibility.

Figure 6(b) shows the T dependence of absorption χ''_{cc} for various frequencies. The absorption χ''_{cc} at $f=0.1$ Hz has a very broad peak around 6–6.5 K, a sharp peak at 10.1 K, and a shoulder around 11.5 K. In the inset we show a plot of the peak temperature around 10.1 K as a function of frequency for $0.1 \leqslant f \leqslant 1000$ Hz. The sharp peak shifts to the high-temperature side with increasing frequency. This peak temperature is close to that of χ'_{aa}.

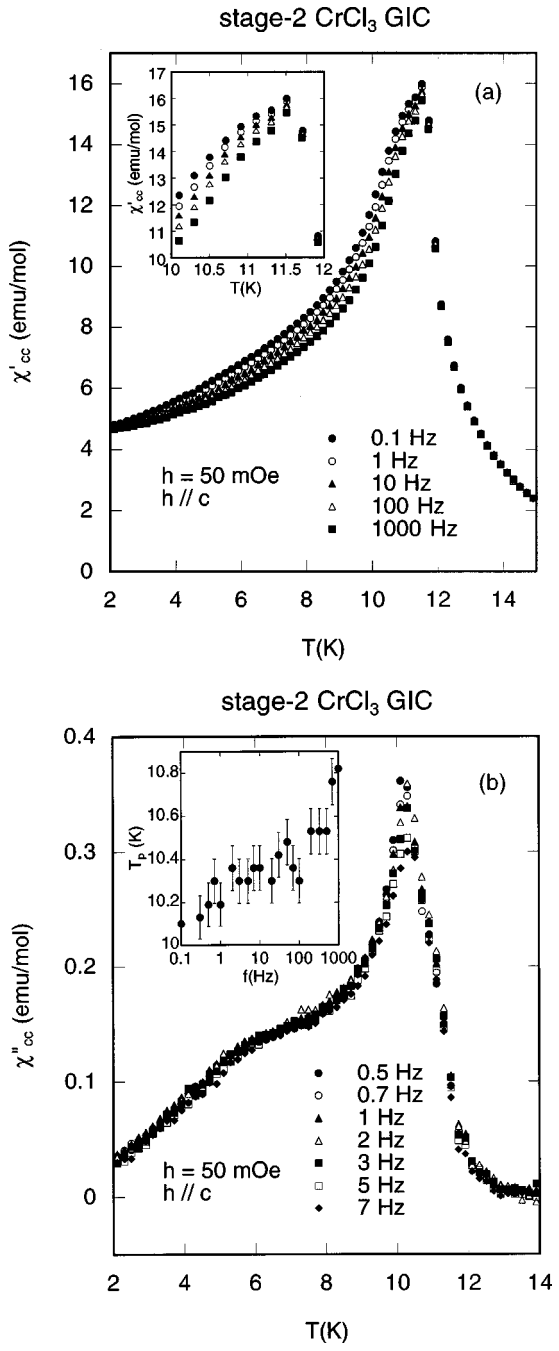

FIG. 6. (a) T dependence of χ'_{cc} for various frequencies f, where $h=50$ mOe, $h\|c$, and $H=0$. The inset shows a detail of χ'_{cc} vs T for $10\leqslant T\leqslant 12$ K. (b) T dependence of χ''_{cc} for various frequencies f, where $h=50$ mOe, $h\|c$, and $H=0$. The inset shows the plot of peak temperature T_p vs f.

F. χ'_{cc} and χ''_{cc} at H

Figure 7(a) shows the T dependence of dispersion χ'_{cc} for various fields applied along the c axis. In Fig. 7(b) we show a plot of the peak temperature as a function of H. The peak temperature decreases with increasing field, having a local minimum around 50–70 Oe, and in turn increases with increasing field. This may be qualitatively explained as follows. In general, the easy-plane-type anisotropy field $H_A^{\rm out}$ is significant to the phase transition of the system with XY spin symmetry. In the absence of an external field, the critical behavior is mainly supported by this field $H_A^{\rm out}$. When the field is applied along the c axis, this symmetry-preserving field decreases to the value of the order of $(H_A^{\rm out}-H)$. For $H<H_A^{\rm out}$ the essential nature of the in-plane spin order does not change, since the field is not a conjugate variable to the two-component order parameter in the easy plane. The in-plane spin order is partly reduced by the field, but is still responsible for the phase transition, leading to the lowering of the peak temperature with increasing H.[19] For $H>H_A^{\rm out}$, however, the spin vector has a component along the c axis and the in-plane component is reduced, giving rise to a crossover of the spin symmetry from XY to Heisenberg character. Once the spins are aligned along the c axis, the ferromagnetic state is enhanced by the application of magnetic field along the c axis. Thus the critical temperature increases with increasing field. In Sec. IV A we show that $H_A^{\rm out}$ is equal to 193 Oe at 1.9 K. The complicated behavior below 100 Oe may be related to the existence of the axial ferromagnetic phase (see Sec. IV C).

Figure 7(c) shows the T dependence of absorption χ''_{cc} for various fields along the c axis, where $f=100$ Hz. The peak around 10.3 K does not shift as the field increases up to 50 Oe and completely disappears at 100 Oe. A very broad peak is observed around 6–7 K for $H=100$ Oe, suggesting the existence of a reentrant spin glass phase (see Sec. IV C).

IV. DISCUSSION

A. Spin Hamiltonian

The spin Hamiltonian of Cr^{3+} in stage-2 $CrCl_3$ GIC may be written as

$$H=-2J\sum_{\langle i,j\rangle}\mathbf{S}_i\cdot\mathbf{S}_j+D\sum_i (S_i^z)^2-2J'\sum_{\langle i,m\rangle}\mathbf{S}_i\cdot\mathbf{S}_m, \quad (7)$$

with $S=3/2$, where J (>0) and J' (<0) are the intraplanar and interplanar exchange interactions, respectively, D (>0) is the single-ion anisotropy, and the z axis coincides with the c axis. Using this Hamiltonian, the in-plane susceptibility (χ_a) and the perpendicular susceptibility (χ_c) can be derived from simple calculations as[20]

$$\chi_a=\frac{N_A(g_a\mu_B)^2}{4k_Bz'|J'|} \quad (8)$$

and

$$\chi_c=\frac{N_A(g_c\mu_B)^2}{k_B(2D+4z'|J'|)}. \quad (9)$$

Since $D>0$ and $J'<0$, χ_a is larger than χ_c. Experimentally, we obtain $\chi_a=M_{\rm FC}^a/H=163.22$ emu/mol and $\chi_c=M_{\rm FC}^c/H=32.48$ emu/mol at $T=1.9$ K. Here, as χ_c, we use the value of 34.23 emu/mol after the correction of demagnetizing effect is taken. Using Eqs. (8) and (9), the parameters D and $z'|J'|$ can be estimated as $D=1.73\times10^{-2}$ K and $z'|J'|=2.30\times10^{-3}$ K. For convenience, these interactions are expressed by the following effective magnetic fields at 0 K: $H_A^{\rm out}=DS/g_c\mu_B=193$ Oe, $H_E=2zJS/g_a\mu_B=393$ kOe, and $H_E'=2z'|J'|S/g_a\mu_B=51$ Oe, where $g_a\approx g_c\approx2$. Note that the value of $H_A^{\rm out}$ is in good agreement with that

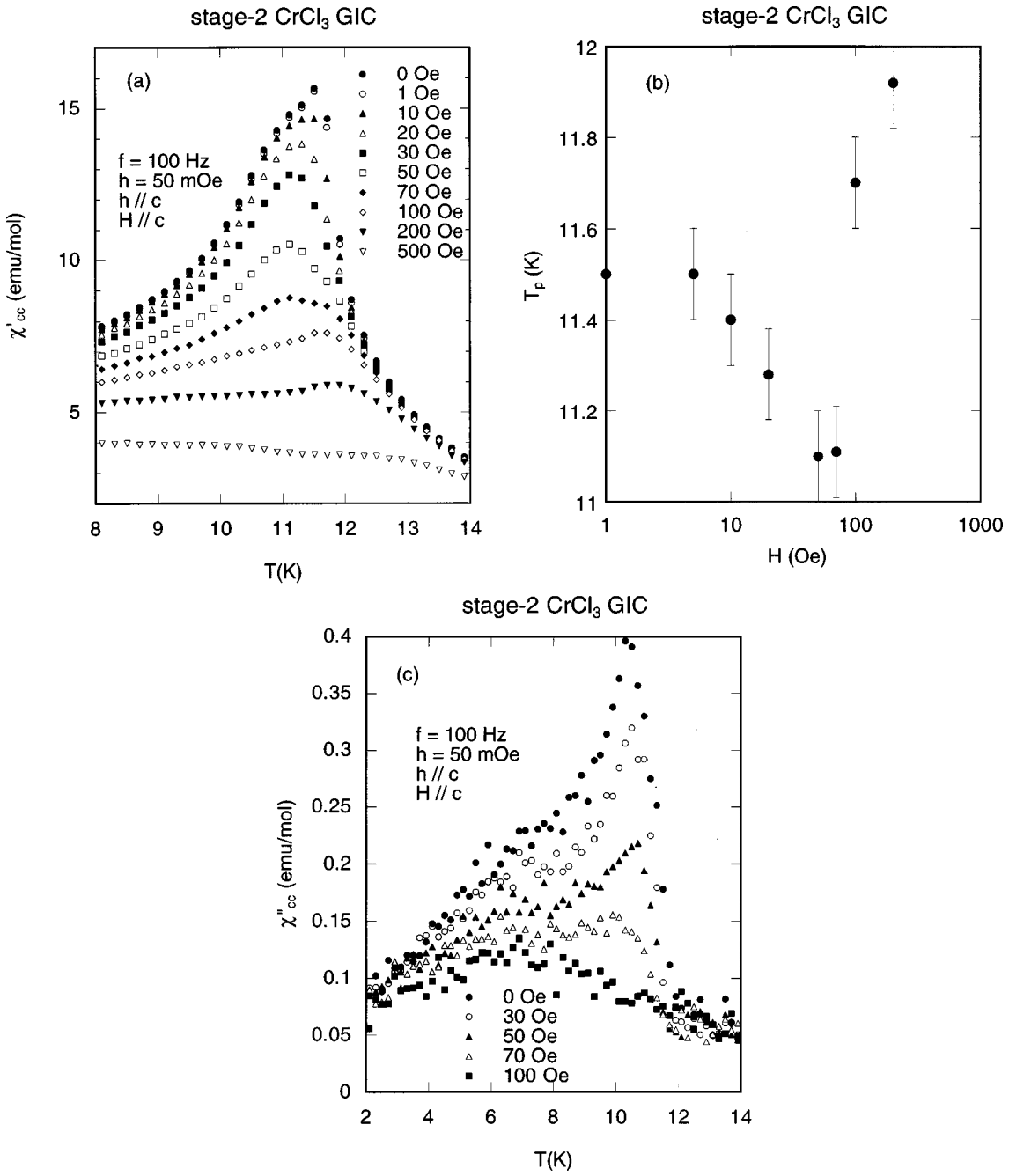

FIG. 7. (a) T dependence of χ'_{cc} for various magnetic fields H ($\|c$) where $f=100$ Hz, $h=50$ mOe, and $h\|c$. (b) Peak temperature T_p vs H. (c) T dependence of χ''_{cc} for various magnetic fields H ($\|c$).

($=200$ Oe) derived from the result of χ_c vs H at 1.9 K [see the inset of Fig. 1(b)]. These effective magnetic fields are compared to those of pristine $CrCl_3$ and K_2CuF_4: $H_A^{\rm out}=2.846$ kOe, $H_E=352$ kOe, and $H'_E=0.84$ kOe for $CrCl_3$ (Ref. 7) and $H_A^{\rm out}=2zJ_AS/g_c\mu_B=2.3$ kOe, $H_E=293$ kOe, and $H'_E=126$ Oe for K_2CuF_4,[17] where J_A is an anisotropic exchange interaction. When $z'=2$ is assumed for stage-2 $CrCl_3$ GIC, the ratio $|J'|/J$ is estimated as 2×10^{-4}, which is much smaller than that of $CrCl_3$ ($=7.8\times10^{-3}$) and is on the same order as that of stage-2 $CoCl_2$ GIC.[2] The degree of XY character defined by the percentage of the ratio $H_A^{\rm out}/H_E$ is 0.05% for stage-2 $CrCl_3$ GIC and 0.8% for both $CrCl_3$ and K_2CuF_4. These results indicate that stage-2 $CrCl_3$ GIC magnetically behaves like a 2D Heisenberg ferromagnet with very small XY anisotropy. The universality class of this compound is close to that of stage-2 $NiCl_2$ GIC.[1]

From the inset of Fig. 1(a), the spin flop field $H_{\rm SF}$ of stage-2 $CrCl_3$ GIC is obtained as $H_{\rm SF}=60$ Oe at 1.9 K. The spin flop field $H_{\rm SF}$ is theoretically predicted as

$$H_{\rm SF}=\left[\frac{2H_A^{\rm in}H'_E}{1-\chi_c/\chi_a}\right]^{1/2}, \tag{10}$$

where $H_A^{\rm in}$ is an anisotropy field in the c plane. Using $H'_E=51$ Oe and $\chi_c/\chi_a=0.21$ at 1.9 K, the field $H_A^{\rm in}$ is estimated as $H_A^{\rm in}=28$ Oe, which is larger than that of pristine $CrCl_3$ ($=10$ Oe).

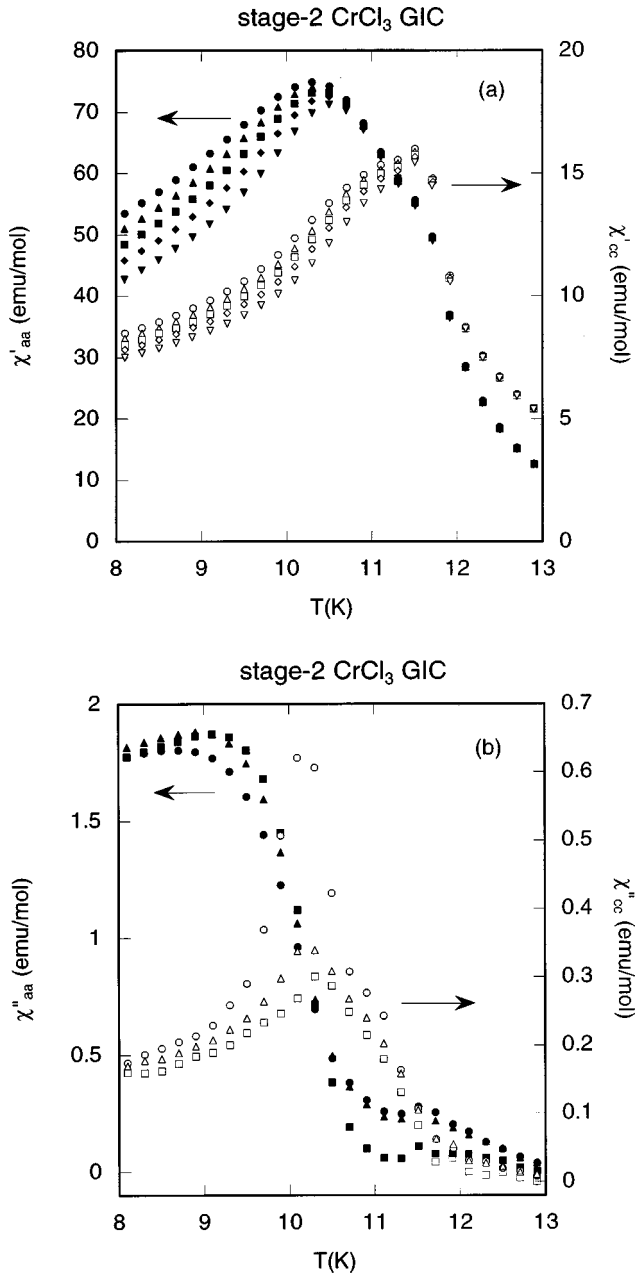

FIG. 8. (a) T dependence of χ'_{aa} and χ'_{cc} with various frequencies. (b) T dependence of χ''_{aa} and χ''_{cc} with various frequencies. $f=0.1$ (●,○), 1 (▲,△), 10 (■,□), 100 (◆,◇), and 1000 (▼,▽) Hz. $h=50$ mOe.

B. Magnetic phase transitions

Before discussing the magnetic phase transitions of this compound, we summarize our results on the T dependence of χ'_{aa}, χ'_{cc}, χ''_{aa}, and χ''_{cc} for stage-2 $CrCl_3$ GIC. To facilitate the comparison, we show the T dependence of the dispersion χ'_{aa} and χ'_{cc} for various frequencies in Fig. 8(a). Clearly, the peak temperature of χ'_{aa} ($=10.3-10.5$ K) is different from that of χ'_{cc} ($=11.5$ K). A kink in χ'_{aa} is observed at 11.5 K. In Fig. 8(b) we show the T dependence of the absorption χ''_{aa} and χ''_{cc}. A broad peak in χ''_{aa} is observed at 8.67–9.70 K depending on frequency and a small peak is observed at 11.5 K. A sharp peak and a small shoulder in χ''_{cc} are observed at 10.3 and 11.5 K, respectively. Furthermore, the absorption χ''_{aa} and χ''_{cc} show anomalies at 5.7–7 K with characteristics of a spin glass phase. These results suggest that the system undergoes four kinds of magnetic phase transitions: T_{c1} ($=11.5$ K), T_{c2} ($=10.3-10.5$ K), T_{c3} ($=8.67-9.70$ K), and T_g ($=5.7-7$ K). The system is in the paramagnetic phase above T_{c1}. A transverse component of spins (along the c axis) orders below T_{c1}, forming a 2D axial ferromagnetic phase. A longitudinal component of spins (along the c plane) orders below T_{c2}, forming a 2D oblique phase where the spin easy axis is slightly tilted from the c plane. A 3D antiferromagnetic long-range order accompanying a spin-glass-like behavior appears below T_{c3}, where the 2D ferromagnetic intercalate layers are antiferromagnetically stacked along the c axis. Below T_g there may be a reentrant spin glass phase. The finite size of small islands formed in the $CrCl_3$ layers is a crucial element in the spin orderings at T_{c2} and T_{c3}. The growth of the in-plane spin correlation length is limited by the existence of islands, making the effective interplanar exchange interaction finite and suppressing the 3D spin ordering to a lower temperature than T_{c2}. At T_{c2} a 2D ferromagnetic spin order develops inside each island. Between T_{c2} and T_{c3} the 2D ferromagnetic long-range order is established. The in-plane spin correlation length grows to the order of the island size, leading to 3D order below T_{c3}. Similar behavior is observed in stage-2 $CoCl_2$ GIC.[2]

Here it is interesting to compare our result of stage-2 $CrCl_3$ GIC with that of stage-3 $CrCl_3$ GIC obtained by Hagiwara *et al.*[11] We believe that the magnetic properties of stage-3 $CrCl_3$ GIC are essentially the same as those of stage-2 $CrCl_3$ GIC. The singularity of nonlinear susceptibility χ_2 is used to examine the nature of long-range order: the sign of χ_2 changes when the spatial magnetic symmetry of the system changes.[21] Hagiwara *et al.*[11] have shown that χ_2 ($f=0.01$, 0.1, and 1 Hz) along the c plane for stage-3 $CrCl_3$ GIC changes its sign from positive to negative at 9.7 K with increasing temperature and has a negative hump around 10.3 K and a negative divergence at 11.4 K. These results indicate that the spatial magnetic symmetry breaking as a whole system occurs only at 9.7 K. The spatial magnetic symmetry is not broken at 10.3 and 11.4 K, because the long-range order may occur within intercalate layers. These results support our result that the 2D spin orders occur at T_{c1} and T_{c2} and that the 3D spin order occurs at T_{c3}. The T dependence of χ_2 below T_{c3} shows no indication of a spin glass phase, which is inconsistent with our result that the reentrant spin glass phase occurs below T_g.

What is the origin of the reentrant spin glass phase below T_g? There is some possibility that a part of Cr^{3+} ions is replaced by Cr^{2+} ions (disproportionation).[12] The charge transfer mechanism in $CrCl_3$ GIC is expected to be similar to that in $FeCl_3$ GIC. Mössbauer spectroscopy measurements of $FeCl_3$ GIC's reveal that almost 20% of Fe ions is Fe^{2+}.[22] If this is true for $CrCl_3$ GIC, it follows that the $CrCl_3$ intercalate layers are formed of a random mixture of Cr^{3+} and Cr^{2+}. There exist three kinds of intraplanar exchange interactions: Cr^{3+}-Cr^{3+}, Cr^{2+}-Cr^{2+}, and Cr^{3+}-Cr^{2+} interactions. The intraplanar exchange interaction between Cr^{2+} spins may be antiferromagnetic because Cr^{2+} spins in pristine $CrCl_2$ are antiferromagnetically coupled with the exchange interaction

J ($=-5.6$ K) within each chain.[23] The spin frustration arising from the competition between ferromagnetic interactions (Cr^{3+}-Cr^{3+}) and possible antiferromagnetic interactions (Cr^{2+}-Cr^{2+}) may lead to the reentrant spin glass phase below T_g.

C. Oblique phase

In stage-2 $CrCl_3$ GIC, χ'_{cc} has a sharp peak and χ'_{aa} has a shoulder at T_{c1}, while χ'_{aa} has a sharp peak and χ'_{cc} shows no anomaly at T_{c2}. A very similar behavior is observed in a 2D random mixture $K_2Cu_cCo_{1-c}F_4$ ($0.95<c<0.98$) with competing orthogonal spin anisotropies.[24] The easy plane (c plane) of Cu^{2+} ions is perpendicular to the easy axis (c axis) of Co^{2+} ions. The interaction between Cu^{2+} spins is ferromagnetic, while the interaction between Co^{2+} is antiferromagnetic. The competition of the orthogonal anisotropies leads to an oblique phase, where the spin easy axis is tilted from the c plane. The dc magnetic susceptibility[24] and neutron scattering[25] clearly show the onset of successive ferromagnetic orderings of transverse and longitudinal spin components at $T_c^{(c)}$ ($=6.0$ K) and $T_c^{(a)}$ ($=4.6$ K), respectively: an axial ferromagnetic phase with the easy spin axis along the c axis between $T_c^{(c)}$ and $T_c^{(a)}$ and an oblique phase below $T_c^{(a)}$. The existence of Co^{2+} ions is crucial to the occurrence of the axial ferromagnetic and oblique phases. These phenomena may be qualitatively explained as follows. At $T_c^{(c)}$, Co^{2+} spins with easy axis ($z\|c$) are ordered. Through the off-diagonal interaction of the form $-2J_0S_i^xS_j^z$, the Cu^{2+} spins are forced to align along the easy axis ($x\|a$) and form an ordered state. When the S^z component is ordered, the molecular field of $J_0\langle S^z\rangle$ is produced on the site of S^x, where $\langle\ \rangle$ denotes the thermal average. This molecular field is not a random field.

How can we explain the successive phase transitions observed in stage-2 $CrCl_3$ GIC? A possible existence of Cr^{2+} is responsible for the axial ferromagnetic and oblique phases. From the similarity of Co^{2+} in $K_2Cu_cCo_{1-c}F_4$, Cr^{2+} spins should have an Ising symmetry with the spin easy axis along the c axis. This is similar to Fe^{2+} with the Ising symmetry in XY-like antiferromagnet $FeCl_3$ GIC. The interaction between Cr^{2+} spins should be antiferromagnetic, which is consistent with the assumption made for the explanation of the reentrant spin glass phase below T_g.

V. CONCLUSION

We have discussed the magnetic phase transitions of stage-2 $CrCl_3$ GIC, which magnetically behaves like a 2D Heisenberg ferromagnet with very small XY anisotropy. This compound undergoes four kinds of magnetic phase transition at T_{c1}, T_{c2}, T_{c3}, and T_g. The role of Cr^{2+} spins with Ising symmetry may be significant to the axial ferromagnetic and oblique phases. The spin frustration effect arising from the competing ferromagnetic (Cr^{3+}-Cr^{3+}) and possible antiferromagnetic (Cr^{2+}-Cr^{2+}) interactions leads to the reentrant spin glass phase below T_g. The assumption of Cr^{2+} ions existing in the intercalate layers is essential to our model. To this end the existence of Cr^{2+} should be confirmed from some direct measurements. Neutron scattering studies are also required in order to examine the spin structure of each phase under a special condition such that the remanent magnetic field be completely removed.

ACKNOWLEDGMENTS

We would like to thank A. W. Moore for providing us with the HOPG sample. This work was partly supported by NSF Grant No. DMR 9625829.

[1] G. Dresselhaus, J. T. Nicholls, and M. S. Dresselhaus, in *Graphite Intercalation Compounds II*, edited by H. Zabel and S. A. Solin (Springer-Verlag, Berlin, 1990).
[2] M. Suzuki, Crit. Rev. Solid State Mater. Sci. **16**, 237 (1990).
[3] C. Starr, F. Bitter, and A. R. Kaufmann, Phys. Rev. **58**, 977 (1940).
[4] W. H. Hansen and M. Griffel, J. Chem. Phys. **28**, 902 (1958).
[5] J. W. Cable, M. K. Wilkinson, and E. O. Wollan, J. Phys. Chem. Solids **19**, 29 (1961).
[6] A. Narath, Phys. Rev. **131**, 1929 (1963).
[7] A. Narath and H. L. Davis, Phys. Rev. **137**, A163 (1965).
[8] J. F. Dillon, Jr., H. Kamimura, and J. P. Remeika, J. Phys. Chem. Solids **27**, 1531 (1966).
[9] B. Kuhlow, Phys. Status Solidi A **72**, 161 (1982).
[10] R. Vangelisti and A. Hérold, Carbon **14**, 333 (1976).
[11] M. Hagiwara, A. Kanaboshi, S. Flandrois, P. Biensan, and M. Matsuura, J. Magn. Magn. Mater. **90&91**, 277 (1990).
[12] D. G. Rancourt, S. Flandrois, P. Biensan, and G. Lamarche, Can. J. Phys. **68**, 1435 (1990).
[13] S. Chehab, P. Biensan, J. Amiell, and S. Flandrois, J. Phys. I **1**, 537 (1991).
[14] S. Flandrois, P. Biensan, J. M. Louis, G. Chouteau, T. Roisnel, G. Andre, and F. Bouree, Mol. Cryst. Liq. Cryst. Sci. Technol., Sect. A **245**, 105 (1994).
[15] S. Chehab, P. Biensan, S. Flandrois, and J. Amiell, Phys. Rev. B **45**, 2844 (1992).
[16] M. Suzuki, J. Phys. Soc. Jpn. **51**, 2772 (1982).
[17] K. Hirakawa, H. Yoshizawa, and K. Ubukoshi, J. Phys. Soc. Jpn. **51**, 2151 (1982); K. Hirakawa, J. Appl. Phys. **53**, 1893 (1982); K. Hirakawa and K. Ubukoshi, J. Phys. Soc. Jpn. **50**, 1909 (1981).
[18] A. Dupas and J.-P. Renard, J. Phys. (Paris), Colloq. **37**, C1-213 (1976).
[19] M. Suzuki and H. Ikeda, J. Phys. Soc. Jpn. **50**, 1133 (1981).
[20] M. E. Lines, Phys. Rev. **131**, 546 (1963).
[21] M. Matsuura and M. Hagiwara, J. Phys. Soc. Jpn. **59**, 3819 (1990).
[22] S. E. Millman and G. Kirczenow, Phys. Rev. B **28**, 5019 (1983).
[23] J. W. Stout and R. C. Chisholm, J. Chem. Phys. **36**, 979 (1962).
[24] M. Itoh, I. Yamada, M. Ishizuka, K. Amaya, T. Kobayashi, K. Koga, and K. Motoya, J. Phys. Soc. Jpn. **59**, 1792 (1990).
[25] H. Kadowaki, H. Yoshizawa, M. Itoh, and I. Yamada, J. Phys. Soc. Jpn. **59**, 713 (1990).